POLITECNICO MILANO 1863

SCUOLA DI INGEGNERIA INDUSTRIALE E DELL'INFORMAZIONE

Nonlinear Dynamics and Chaos

Project report: An hybrid averaging and harmonic balance method for weakly nonlinear asymmetric resonators

Authors:

Barutta E.	10726132
Milic K.	11012938
Visentin N.	10797203

Lecturers:
Jain S.
Marconi J.

Academic Year: 2023/24

Contents

1 Introduction **3**

2 Hybrid method **3**

2.1 Model and assumptions 3

2.2 Harmonic extraction 4

2.3 Averaging 5

3 Response analysis **6**

3.1 Steady-state solution 6

3.2 Stability and bifurcations 7

4 Analysis of the results **8**

5 Conclusions **10**

1 Introduction

This report discusses a particular method for studying weakly nonlinear systems, involving harmonic balance and averaging techniques, presented by Steven W. Shaw, Oriel Shoshani and Sahar Rosenberg [1].

There are many different ways to mathematically describe equation of motion of a physical system, ranging from simple to more complex models. A common choice consists in including only quadratic and cubic nonlinear stiffness terms, however the resulting asymmetric system is not able to catch any possible non-monotonic behaviour of the physical response, at least when a low order perturbation method is employed. One other possibility is using only cubic and quintic terms, which also allows to describe non-monotonic behaviours:

$$\ddot{x}(t) + \omega_0^2 x(t) + \gamma x^3(t) + \sigma x^5(t) = 0 \quad , \quad \gamma\sigma < 0 \tag{1}$$

On the other hand, these symmetric model looses connection with the asymmetric physics of the real system.
Taking into account both symmetric and asymmetric terms, up to quintic order, gives a more accurate description of the behaviour of the system:

$$\ddot{x}(t) + \omega_0^2 x(t) + k_2 x^2(t) + k_3 x^3(t) + k_4 x^4(t) + k_5 x^5(t) = 0$$

However, this results in cumbersome expressions to analyze, increasing the complexity of the model and requiring very computational intensive procedures, such as multiple scales method involving many time scales, or averaging with a lot of coordinate changes, or even global methods for strongly nonlinear systems.[2] [3]

The "hybrid method" presented in the paper allows to deal in a relatively simple way with this more complicated model by "merging" high-order harmonic balance and first-order time averaging. The main difference from the previously mentioned approaches is that it is able to catch accurate information about high order harmonics without dealing with heavy calculations. Moreover, it maintains the physical connection between the coefficients in the model and the physical system. However, due to the introduction of the low-order approximation, this method is not able to correctly describe the transient dynamics, but only the steady-state condition. Finally, we can conclude that this hybrid method is more numerically intensive than perturbation methods, but it's easier than "brutal" numerical methods for parametric analysis.

2 Hybrid method

2.1 Model and assumptions

We will focus on a very generic single mode weakly nonlinear system which can be described by the following equation of motion:

$$\ddot{x}(t) + 2\Gamma g(x(t))\dot{x}(t) + \omega_0^2 x(t) + f(x(t)) = h(x) F \cos(\Omega t) \tag{2}$$

where:

ω_0 is the mode eigenfrequency;

Γ describes the linear damping;

$g(x) = 1 + g_1 x + g_2 x^2 + g_3 x^3 + g_4 x^4$ takes into account nonlinear damping effects up to the fourth order;

$f(x) = 1 + \alpha_2 x^2 + \alpha_3 x^3 + \alpha_4 x^4 + \alpha_5 x^5$ describes the nonlinear stiffness terms up to the quintic order;

$h(x) = 1 + h_1 x + h_2 x^2$ represents nonlinear displacement-dependant excitation;

F is the forcing amplitude and Ω is the forcing frequency.

It is noteworthy to mention that, even if the studied system is quite general, the method can be applied to other systems, where $g(x)$, $f(x)$ and $h(x)$ can assume different forms and also depend on $\dot{x}$.
The response of the system, for energy levels associated with weakly nonlinear dynamics, can be expressed as:

$$x(t) = \varepsilon \cdot a(t) \cdot cos(\Omega t + \phi) + a_0(t) + \sum_{k=2}^{5} a_k(t) \cdot cos(k\Omega t + k\phi(t)) \tag{3}$$

where the energy of the overtones ($k = 2, 3, 4, 5$) and of the constant offset (a_0) is much lower than the one of the fundamental harmonic. a_k coefficients are assumed to be polynomial functions of εa:

$$\begin{aligned}
a_0 &= c_{02} \cdot (\varepsilon a)^2 + c_{04} \cdot (\varepsilon a)^4 \\
a_2 &= c_{22} \cdot (\varepsilon a)^2 + c_{24} \cdot (\varepsilon a)^4 \\
a_3 &= c_{33} \cdot (\varepsilon a)^3 + c_{35} \cdot (\varepsilon a)^5 \\
a_4 &= c_{44} \cdot (\varepsilon a)^4 \\
a_5 &= c_{55} \cdot (\varepsilon a)^5
\end{aligned} \tag{4}$$

From now on, it is assumed that:

- $a = a(\varepsilon^4 t)$
- $\phi = \phi(\varepsilon^4 t)$
- $\Gamma = \varepsilon^4 \tilde{\Gamma}$
- $\Omega = \omega_0 + \varepsilon^4 \Delta\omega$
- $F = \varepsilon^5 \tilde{F}$

The first two assumptions mean that the amplitude and the phase of the fundamental harmonic are slowly varying with respect to time, implying that they are basically constant within one oscillation, while the other hypothesis derive from the weakly nonlinearity of the system.
Deriving (3) and applying the standard constraint for averaging:

$$\dot{a}\ cos(\Omega t + \phi) - a\ \dot{\phi}\ sin(\Omega t + \phi) = 0 \tag{5}$$

leads to:

$$\dot{x} = -\varepsilon \Omega a sin(\Omega t + \phi) - \Omega \sum_{k=2}^{5} a_k k\ sin(k(\Omega t + \phi)) \tag{6}$$

Then deriving again this last equation we obtain:

$$\ddot{x} = -\varepsilon^5 \Omega \dot{a} sin(\Omega t + \phi) - \varepsilon^5 \Omega (\frac{\Omega}{\varepsilon^4} + \dot{\phi}) a cos(\Omega t + \phi) - \Omega^2 \sum_{k=2}^{5} a_k k^2 cos(k(\Omega t + \phi)) \tag{7}$$

Note that all terms of order higher than ε^5 are removed.

2.2 Harmonic extraction

To find coefficients c_{kj} in equation (4), equations (3), (4) (6), (7) are substituted into (2) and all the terms are expanded with a script able to perform symbolic operations.
Next, a parallelization tool can be employed to extract simultaneously the coefficients for each harmonic, i.e. the constant terms and the coefficients of $cos(2(\Omega t + \phi))$, $cos(3(\Omega t + \phi))$, $cos(4(\Omega t + \phi))$ and $cos(5(\Omega t + \phi))$. After that, a similar algorithm is used to collect all the coefficients sharing the same power of ε from the second up to the fifth power, which are then set to zero.
This results in a set of 20 equations, though most are identities. By neglecting those, a system of 8 nonlinear equations is

obtained. Solving this system yields the desired coefficients:

$$
\begin{aligned}
a_0 &= -(\epsilon a)^2 \, \frac{\alpha_2}{2\omega_0^2} - (\epsilon a)^4 \left(\frac{19\alpha_2^3 - 45\omega_0^2\alpha_2\alpha_3 + 27\omega_0^4\alpha_4}{72\omega_0^6} \right) \\
a_2 &= (\epsilon a)^2 \, \frac{\alpha_2}{6\omega_0^2} - (\epsilon a)^4 \left(\frac{14\alpha_2^3 + 45\omega_0^2\alpha_2\alpha_3 - 48\omega_0^4\alpha_4}{28\omega_0^6} \right) \\
a_3 &= (\epsilon a)^3 \left(\frac{2\alpha_2^2 + 3\omega_0^2\alpha_3}{96\omega_0^4} \right) - (\epsilon a)^5 \left(\frac{580\alpha_4^4 + 3240\omega_0^2\alpha_2^2\alpha_3 - 405\omega_0^4\alpha_3^2 + 648\omega_0^4\alpha_2\alpha_4 - 540\omega_0^6\alpha_5}{69120\omega_0^8} \right) \\
a_4 &= (\epsilon a)^4 \left(\frac{10\alpha_2^2 + 45\omega_0^2\alpha_2\alpha_3 + 36\omega_0^4\alpha_4}{4320\omega_0^6} \right) \\
a_5 &= (\epsilon a)^5 \left(\frac{14\alpha_2^2\alpha_3 + 9\omega_0^2\alpha_3^2 + 32\omega_0^2\alpha_2\alpha_4 + 24\omega_0^4\alpha_5}{9216\omega_0^6} \right)
\end{aligned} \tag{8}
$$

Thanks to the previous assumptions, these equations are totally independent from the damping and forcing terms. Therefore, they are able only to properly capture the effects of stiffness nonlinearities.

2.3 Averaging

After deriving the polynomial expressions for each a_k using the harmonic balance method, averaging can be applied more easily compared to applying it directly to the original equation of motion.
Substituting (8) into (3), (6), (7) and then inserting the resulting expressions of x, $\dot{x}$ and $\ddot{x}$ in (2) gives the equation of motion written in the new coordinates $a(t)$ and $\phi(t)$. Note that it contains terms up to order ε^{25}, but everything above order ε^5 is removed. Taking this equation together with the constraint equation (5) and solving for $\dot{a}$ and $\dot{\phi}$ leads to a set of two ODEs that rule the dynamics of $a(t)$ and $\phi(t)$. These equations can then be averaged (by means of the integral average over the period $T = \frac{2\pi}{\Omega}$), obtaining, for $\varepsilon = 1$:

$$
\begin{cases}
\dot{\bar{a}} = -\Gamma \bar{a} - \frac{F}{2\omega_0} sin(\bar{\phi}) \\
\dot{\bar{\phi}} = \omega_0 - \Omega + \frac{3}{8}\frac{\gamma_{eff}}{\omega_0}\bar{a}^2 + \frac{5}{16}\frac{\sigma_{eff}}{\omega_0}\bar{a}^4 - \frac{F}{2\bar{a}\omega_0} cos(\bar{\phi})
\end{cases} \tag{9}
$$

with:

$$
\begin{aligned}
\gamma_{eff} &= \alpha_3 - \frac{10}{9}\left(\frac{\alpha_2}{\omega_0}\right)^2 \\
\sigma_{eff} &= \alpha_5 - \frac{11}{12}\left(\frac{\alpha_2^2}{\omega_0^3}\right)^2 + \frac{53\alpha_3}{20}\left(\frac{\alpha_2}{\omega_0^2}\right)^2 - \frac{14\alpha_2\alpha_4}{5\omega_0^2} + \frac{3}{80}\left(\frac{\alpha_3}{\omega_0}\right)^2
\end{aligned}
$$

Equations (9) regulate the slow dynamics of $a(t)$ and $\phi(t)$, in fact they tell us how the averaged quantities $\bar{a}(t)$ and $\bar{\phi}(t)$ vary in time, while the fast oscillations are removed by averaging during one cycle. Note that, for simplicity, from the next section the notation $\bar{a}(t)$ and $\bar{\phi}(t)$ is reduced to $a(t)$ and $\phi(t)$.

Observe that equations (9) are exactly the same one would obtain by applying a "classical" averaging procedure on a simpler system such as (1), but in that case the expression of γ_{eff} and σ_{eff} would simply be γ and σ. The same applies to a model with only quadratic and cubic nonlinear terms, again with a different form of γ_{eff} and σ_{eff}.
Moreover, as expected, equations (9) correctly show a slow variation, i.e. $\mathcal{O}(\varepsilon^4 t)$, of $\bar{a}(t)$ and $\bar{\phi}(t)$, since $\Delta\omega$, F and Γ are assumed to be small. However, the second equation reveals the presence of an intermediate time scale $\mathcal{O}(\varepsilon^2 t)$, which is neglected in this analysis, meaning that it is assumed to have ended its transient while we only study the evolution of the slowest scale $\mathcal{O}(\varepsilon^4 t)$:

$$
\begin{aligned}
\bar{a} &= \bar{a}(\varepsilon^2 t \to +\infty, \varepsilon^4 t) \\
\bar{\phi} &= \bar{\phi}(\varepsilon^2 t \to +\infty, \varepsilon^4 t)
\end{aligned}
$$

As a consequence of that, equations (9) are able to provide a good enough approximation of the solution only near fixed points, limited to regime conditions.

3 Response analysis

3.1 Steady-state solution

The steady-state response of the system is determined by setting $(\dot{a}, \dot{\phi}) = (0, 0)$ from (9).

$$\begin{cases} 0 = -\Gamma a - \frac{F}{2\omega_0} sin(\phi) \\ 0 = \omega_0 - \Omega + \frac{3}{8}\frac{\gamma_{eff}}{\omega_0}a^2 + \frac{5}{16}\frac{\sigma_{eff}}{\omega_0}a^4 - \frac{F}{2a\omega_0}cos(\phi) \end{cases}$$

$$\begin{cases} sin(\phi) = -\Gamma a \frac{2\omega_0}{F} \\ cos(\phi) = \left(\omega_0 - \Omega + \frac{3}{8}\frac{\gamma_{eff}}{\omega_0}a^2 + \frac{5}{16}\frac{\sigma_{eff}}{\omega_0}a^4\right)\frac{2a\omega_0}{F} \end{cases} \tag{10}$$

From the last expression, the value of $tan(\phi_{ss})$ can be obtained by dividing $sin(\phi)$ by $cos(\phi)$ and an implicit formulation for a_{ss} is found by raising to the second power both equations and summing them up.

$$a_{ss}^2 = \left(\frac{F}{2\omega_0}\right)^2 \left[\Gamma^2 + \left(\omega_0 - \Omega + \frac{3}{8}\frac{\gamma_{eff}}{\omega_0}a_{ss}^2 + \frac{5}{16}\frac{\sigma_{eff}}{\omega_0}a_{ss}^4\right)^2\right]^{-1} \tag{11}$$

$$tan(\phi_{ss}) = \Gamma\left[\Omega - \omega_0 - \frac{3}{8}\frac{\gamma_{eff}}{\omega_0}a_{ss}^2 - \frac{5}{16}\frac{\sigma_{eff}}{\omega_0}a_{ss}^4\right]^{-1} \tag{12}$$

The results of these two equations are, respectively, the steady-state amplitude a_{ss} and the steady-state phase ϕ_{ss}.

Resonance Now we want to find the resonance amplitude a_{res}, i.e. the biggest value of a_{ss} on the response curve given a certain value of F, and the resonance frequency ω_{res}, i.e. the corresponding natural frequency of the nonlinear system. To obtain ω_{res} it's sufficient to impose the resonance condition $\phi_{res} = -\pi/2$ in equation (12) and solve it for Ω:

$$tan\left(-\frac{\pi}{2}\right) \to \infty \implies \Omega - \omega_0 - \frac{3}{8}\frac{\gamma_{eff}}{\omega_0}a_{ss}^2 - \frac{5}{16}\frac{\sigma_{eff}}{\omega_0}a_{ss}^4 = 0$$

$$\omega_{res} = \omega_0 + \frac{3}{8}\frac{\gamma_{eff}}{\omega_0}a_{res}^2 + \frac{5}{16}\frac{\sigma_{eff}}{\omega_0}a_{res}^4 \tag{13}$$

This equation is also able to provide a very good approximation for the backbone curves: as we can see, the natural frequency of the nonlinear system changes as the amplitude varies, following different possible behaviours (hardening, softening, non-monotonic) in function of the value of the parameters.
To get a_{res}, we can impose $\Omega = \omega_{res}$ in equation (11) using (13) and then solve for a_{ss}. The resulting amplitude is the resonance amplitude a_{res}:

$$a_{res} = \frac{F}{2\omega_0\Gamma} \tag{14}$$

Non-monotonic behaviour As we previously mentioned, equation (13) provides an expression for the backbone curves. This approximation can be compared with the known results from a system with only quadratic and cubic nonlinearities, resulting in very similar curves. Moreover, as we can see from (13), this formula is also able to describe a generic non-monotonic behaviour.
Additionally, these results can be used to find out if a non-monotonic tendency arises. In particular there are two conditions that need to be satisfied for that to happen:

- Existence of a zero-dispersion (ZD) point $\to$ this requires, for the unforced undamped system, $\frac{\partial\omega_{res}}{\partial a_{res}}\Big|_{a_{res}\neq 0} = 0$

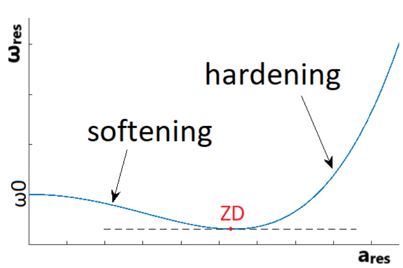

imposing the derivative of (13) to zero: $a_{zd} = \sqrt{-\frac{3}{5}\frac{\gamma_{eff}}{\sigma_{eff}}}$ (15)

substituting a_{zd} into (13): $\omega_{zd} = \omega_0 - \frac{9}{80}\frac{\gamma_{eff}^2}{\omega_0\sigma_{eff}}$ (16)

- For the forced system, a big enough value of the forcing amplitude F that "triggers" this behaviour. In particular, we need F such that $a_{res} > a_{zd}$

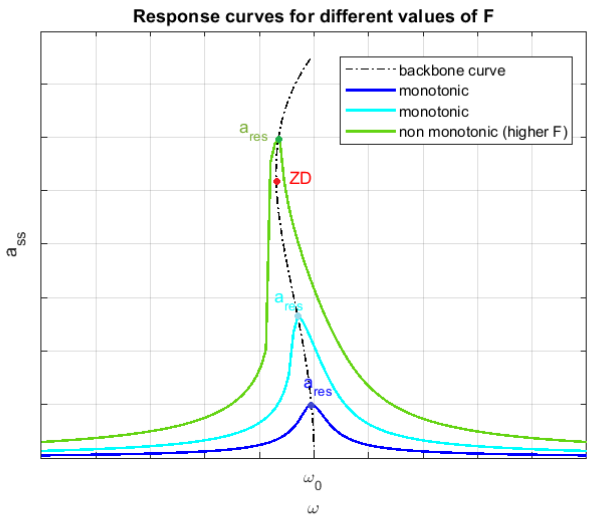

imposing $a_{res} > a_{zd}$ using (14) and (15) we can easily find:

$$F > 2\omega_0 \Gamma \sqrt{-\frac{3}{5}\frac{\gamma_e f f}{\sigma_e f f}} \tag{17}$$

3.2 Stability and bifurcations

To address the stability of the different branches of the response curve, a perturbation is introduced around the steady-state conditions. Taking equation (9) and linearizing around (a_{ss}, ϕ_{ss}) from (11) and (12), and then substituting (10) in the obtained expression, leads to the following Jacobian:

$$\mathbf{J} = \begin{bmatrix} -\Gamma & a_{ss}\left(\Omega - \omega_0 - \frac{3\gamma_{eff}}{8\omega_0}a_{ss}^2 - \frac{5\sigma_{eff}}{16\omega_0}a_{ss}^4\right) \\ -\frac{1}{a_{ss}}\left(\Omega - \omega_0 - \frac{9\gamma_{eff}}{8\omega_0}a_{ss}^2 - \frac{25\sigma_{eff}}{16\omega_0}a_{ss}^4\right) & -\Gamma \end{bmatrix}$$

The trace and the determinant of this matrix can be used to develop quantitative calculation on this matter:

$$tr(\mathbf{J}) = -2\Gamma \tag{18}$$

$$det(\mathbf{J}) = \Gamma^2 + \left(\Omega - \omega_0 - \frac{3\gamma_{eff}}{8\omega_0}a_{ss}^2 - \frac{5\sigma_{eff}}{16\omega_0}a_{ss}^4\right)\left(\Omega - \omega_0 - \frac{9\gamma_{eff}}{8\omega_0}a_{ss}^2 - \frac{25\sigma_{eff}}{16\omega_0}a_{ss}^4\right)$$

Looking at (18), it is evident that the trace is null only if the system is conservative, i.e. $\Gamma = 0$, but in the most general case, this is not true and implies that no Hopf bifurcations can occur. In fact, to appear, this type of bifurcation requires a pair of purely imaginary eigenvalues [2]. In our case the eigenvalues are:

$$\lambda_{1,2} = -\Gamma \pm j\frac{\sqrt{\cdots}}{2}$$

thus, the only way to get a Hopf bifurcation is, once again, having $\Gamma = 0$.
Instead, a static bifurcation can appear only in case the system has a null eigenvalue [2], which means that

$$det(\mathbf{J}) = 0 \tag{19}$$

is satisfied. The type of bifurcation in this case can be determined by the system's response curve. In our scenario, the curve indicates the presence of only a saddle-node bifurcation, as it shows an infinite slope in the response plot ($\frac{da_{ss}}{d\omega} \to \infty$). However, the rise of these branches is possible, as previously said, only if a critical value of the forcing is reached [4]. By rearranging (19) and substituting the resulting expression into (11), we obtain the following expression, which describes the force amplitude and holds at bifurcation points (ω_{sn}, a_{sn}):

$$\left(\frac{F}{2\omega_0}\right)^2 = a_{sn}^4\left(\frac{3\gamma_{eff}}{4\omega_0} + \frac{5\sigma_{eff}}{4\omega_0}a_{sn}^2\right)\left(\omega_{sn} - \omega_0 - \frac{3}{8}\frac{\gamma_{eff}}{\omega_0}a_{sn}^2 - \frac{5}{16}\frac{\sigma_{eff}}{\omega_0}a_{sn}^4\right) \tag{20}$$

The critical value of the force is obtained by setting $\frac{dF^2}{da_{sn}^2} = 0$ from (20). An expression for a_{sn}^2 is obtained, which unfortunately still depends on ω_{sn}. To solve this problem, the result is substituted in (19) and the critical value of the force is obtained from (20). In the particular case in which $\sigma_{eff} = 0$, i.e. only effective cubic nonlinearities, the final simplified expression is given by:

$$F_{cr} = \sqrt{\frac{256\omega_0^2\Gamma^3}{9\sqrt{3}|\gamma_{eff}|}}$$

4 Analysis of the results

All the passages presented in section 2 were reproduced using the symbolic environment in MatLab and the results in section 3 were analysed as well.

First of all, we have noticed that the coefficients c_{35} and c_{55} found by solving the harmonic balance equations result slightly different to the ones presented in the paper [1] and shown in (4):

$$c_{35} = -\left(\frac{580\alpha_4^4 + 3240\omega_0^2\alpha_2^2\alpha_3 - 405\omega_0^4\alpha_3^2 + 648\omega_0^4\alpha_2\alpha_4 - 2700\omega_0^6\alpha_5}{69120\omega_0^8}\right)$$
$$c_{55} = \left(\frac{100\alpha_2^4 + 900\omega_0^2\alpha_2\alpha_3 + 1584\omega_0^4\alpha_4\alpha_2 + 405\alpha_3^2\omega_0^4 + 1080\alpha_5\omega_0^6}{414720\omega_0^8}\right)$$

However, this does not influence the following computations at all.
Fixing $\alpha_3 = 1$, $\alpha_4 = \alpha_5 = 0$, and $\omega_0 = 10$ it is possible to represent the backbones curves (*figure* 1) for different values of α_2 using (13):

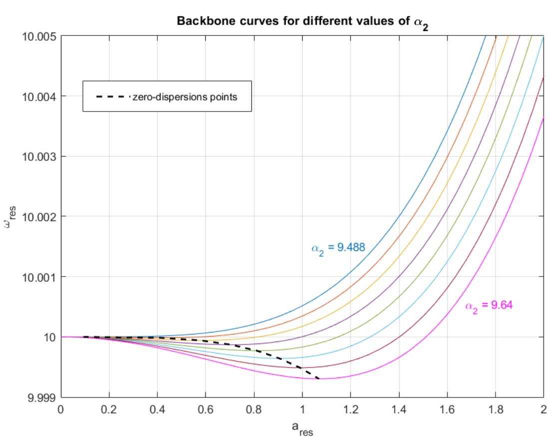

Figure 1: Backbone curves for different values of α_2

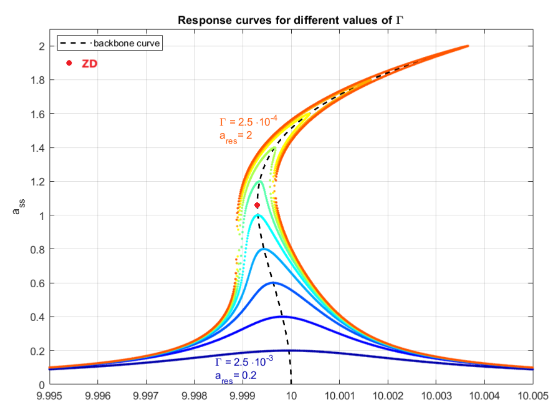

Figure 2: Response curves for different values Γ

Notice how the non-monotonic behaviour rises only for certain values of α_2. Moreover, even if we are limiting our model to quadratic and cubic nonlinearities ($\alpha_4 = \alpha_5 = 0$), the hybrid method is still able to describe mixed softening and hardening. The black dashed line is the locus of the zero-dispersion points (plotted using (15) and (16) for different α_2).
Passing to the forced system, with $F = 0.01$, $\alpha_2 = 9.64$ and maintaining the other parameters as before, by using equation (11) we can plot the response curves for different values of Γ ($\Gamma = \frac{F}{2\omega_0 a_{res}}$) such that $a_{res} = [0.2, 2]$ (*figure* 2). As we can see from the image, when a_{res} is bigger than a_{zd} the non-monotonic behaviour appears, similarly to what is expressed in (17) for the force. Moreover, if the amplitude is increased even more, two other real solutions show up, which graphically means a triple intersection with a vertical line and analytically the manifestation of the saddle-node bifurcation.
Alternatively, it is possible to set $\Gamma = 3 \cdot 10^{-4}$ and let α_3 to vary within the range $[0.95, 1.05]$:

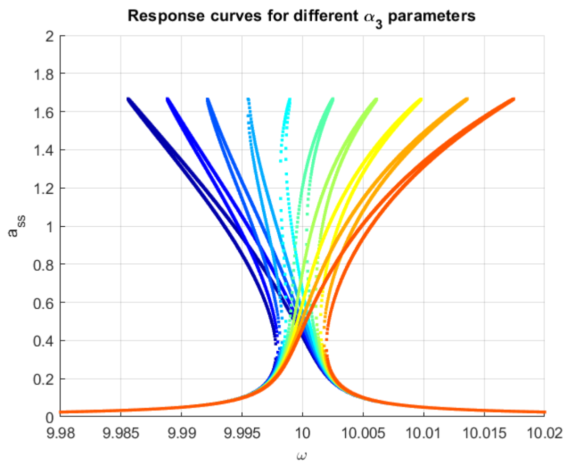

Figure 3: Response curves for different values α_3

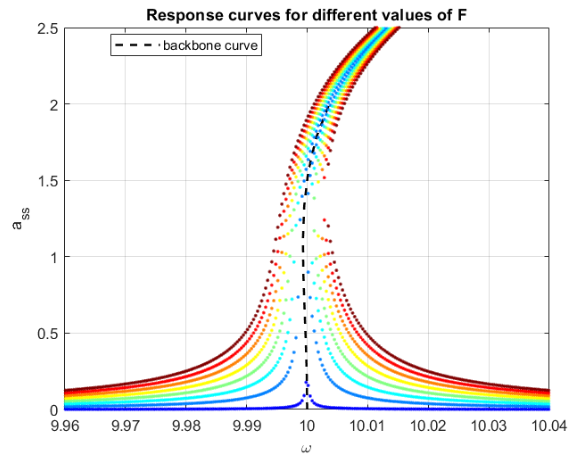

Figure 4: Response curves for different values of F

In *figure* 3, we can see that the response changes, as expected, from a softening to a hardening behaviour when the value of the cubic term increases in magnitude. Instead, in *figure* 4 we decided to plot the response curve, fixing all the parameters but varying the magnitude of F. As result the shape of the curve is not varying while its width extremely depends on the value of the force.

We also tried to numerically simulate the system, solving equation (2) with $\omega_0 = 10$, $\alpha_2 = 9.64$, $\alpha_3 = 1$, $\alpha_4 = \alpha_5 = 0$, $\Gamma = 2.5 \cdot 10^{-4}$, $F = 0.01$, $\Omega = 10.003$ (or $\Omega = 9.998$, which gives similar results) and $x(0) = 0.1$, $\dot{x}(0) = 0$ as initial conditions. ode45 solver from MatLab was employed.

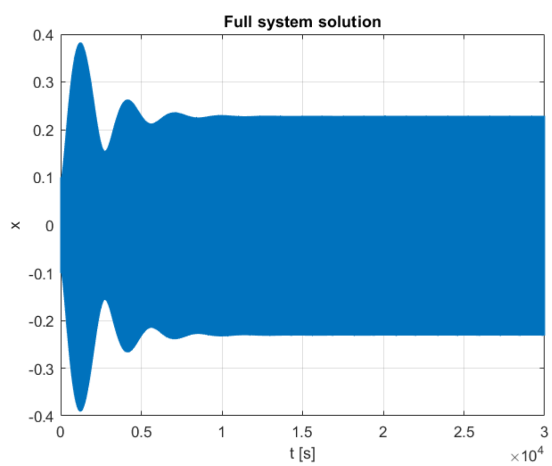

Figure 5: Full time response

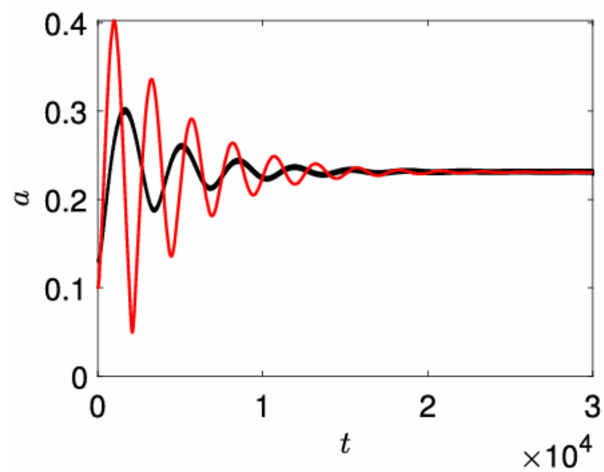

Figure 6: Transient analysis covered in [1]. Black: numerical simulation, red: hybrid method

As we can see from *figure* 5, after a long transient, the response seems to stabilize with an oscillating amplitude of more or less 0.23. This result is quite consistent with the transient analysis in the appendix of [1], which was developed using the same parameters, showing the incapability of the hybrid method to catch the non-regime dynamics (*figure* 6).
On the other hand, *figure* 7 shows the frequency content of the regime solution (black curve; the last 10% of the time response was considered). The amplitude of the main harmonic is found to be $a_{res} \simeq 0.22$, which is consistent with *figure* 6. From here, the magnitude of the overtones and DC term can be estimated using the results provided in expressions (8), that are graphically represented in *figure* 8. The corresponding theoretical values for a_k are then reported in *figure* 7 (red, green, purple, yellow, light blue and pink lines) for a comparison with the experimental results.

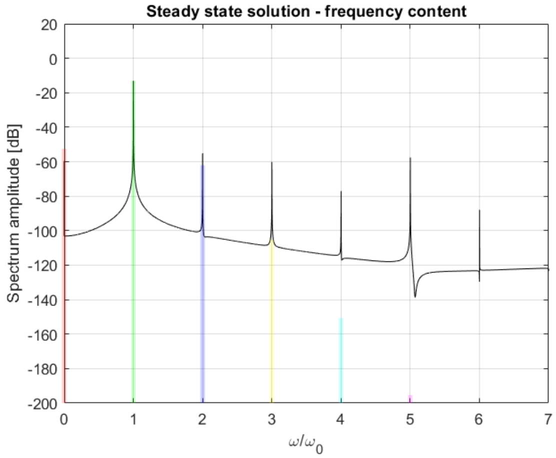

Figure 7: Spectrum of the regime solution

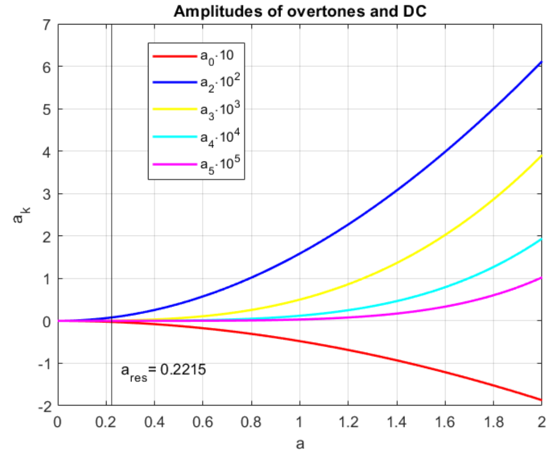

Figure 8: Amplitude of the overtones and DC term as functions of the main harmonic amplitude a

While the hybrid method gives a good approximation for a_0 and a_2, the higher harmonics are not so well reconstructed. Moreover, even if the system parameters were the same, there is a substantial discrepancy with respect to the main response amplitude found numerically in the paper [1], where $a_{res} = 1.92$. However, this last result is close to the estimation provided by the hybrid method in (14), that leads to $a_{res} = 2$.

5 Conclusions

This report provides a discussion of a hybrid method that combines harmonic balance with first-order averaging, offering a relatively accurate and straightforward approach to manage weakly nonlinear systems containing higher-order nonlinearities.

By employing this method, it is possible to adopt a more refined model of the physical system, improving the precision of the analysis without increasing the computational burden too much. This trade off between accuracy and computational efficiency is important, in particular, in complex systems where higher-order effects cannot be neglected. Moreover, this hybrid method also provides a more refined solution in the case of low order nonlinear stiffness terms, where classical "simple" approaches are not able to describe a non-monotonic behaviour.

However, the method presents some limitations. The most significant drawback is its impossibility to capture the transient behavior of the response and the capability of only studying the steady-state condition. Additionally, as discussed in section 2.3, the results obtained through this method are only valid in regions very close to the fixed points of the system.

In Section 3, we have tried to reproduce the calculation developed in the paper with a symbolic environment but, during this process, we found some discrepancies between the theoretical results and the ones obtained through symbolic computation. Nevertheless, we were able to find proper response curves as functions of some relevant varying parameters and to analyze correctly the stability and bifurcations of different branches of the regime solution.

Finally, as suggested in the paper [1], it would be possible to modify the hybrid procedure, either by adapting it to work with systems that have a different form from (2), or by implementing some higher-order perturbation methods to have a correct analysis also for the transient dynamics.

References

[1] Steven Shaw, Sahar Rosenberg, and Oriel Shoshani. "A hybrid averaging and harmonic balance method for weakly nonlinear asymmetric resonators". In: (June 2022). DOI: 10.21203/rs.3.rs-1789782/v1.

[2] Philip Holmes John Guckenheimer. Nonlinear Oscillations, Dynamical Systems, and Bifurcations of Vector Fields. Vol. 1. New York: Springer New York, NY, 2013.

[3] Steven H. Strogatz. Nonlinear Dynamics and Chaos: With Applications to Physics, Biology, Chemistry and Engineering. Westview Press, 2000.

[4] E. M. Lifshitz L. D. Landau. Mechanics. Vol. 1. New York: Elsevier, 1982.